

## Some Physical Properties of Mesoscale Eddies in the Caspian Sea Basins Based on Numerical Simulations

Rahnemania, A.<sup>1</sup>, Aliakbari-Bidokhti, A. A.<sup>2\*</sup> and Babagoli Matikolaei, J.<sup>3</sup>

1. Ph.D. Graduated, Department of Space Physics, Institute of Geophysics, University of Tehran, Tehran, Iran

2. Professor, Department of Space Physics, Institute of Geophysics, University of Tehran, Tehran, Iran

3. M.Sc. Graduated, Department of Space Physics, Institute of Geophysics, University of Tehran, Tehran, Iran

(Received: 15 Feb 2021, Accepted: 25 May 2021)

### Abstract

This paper investigates the mechanism of the eddy's formation and their locations in the Caspian Sea using numerical simulations. The HYCOM model is used to simulate the evolutions of eddies. The model ran for 18 years from 1992 to 2009 while river runoff and atmospheric forcing are applied in the model as input files. The model output is appropriately compared to some observation data. The results indicate that one cyclonic eddy in the middle and two cyclonic and anticyclonic eddies in the southern basin of the Caspian Sea are the main eddies in this closed sea. Herein we prepare a comprehensive map to show the exact location of eddies with their important features like scales of them in all months using model simulation outputs. Topographic steering seems to be very important in the formation of mesoscale deep basin size eddies.

**Keywords:** HYCOM, Numerical modelling, Mesoscale eddies, Caspian Sea.

### 1. Introduction

In geophysical fluid dynamics, an eddy can be described as the swirling of a fluid while the fluid is unstable or in a turbulent flow regime. Eddies are very important for oceanographers as they advect momentum, heat, and mass (Gill, 1983). This importance would be much more important in a closed basin like the Caspian Sea.

The Caspian Lake (or Sea) is an enclosed basin with low salinity water (Kostianoy et al., 2005; Babagoli Matikolaei et al., 2017), extending in the north-south direction. In terms of water area and volume, it is the greatest lake in the world, which is located roughly 27 below mean sea level (Aubrey, 1994). While the whole coastline of this sea can be estimated as 7000 km, 922 km is located on the Iranian coast (Aubrey et al., 1994). The areas of northern, middle, and southern basins are 8000, 13800, and 164800 km<sup>2</sup> respectively (Kosarev, 1990; Rodionov, 2012; Terziev et al., 1992; Zonn et al., 2010). Calculations show that the volume of the Caspian Sea is nearly 66780 km<sup>3</sup> that is approximately 44% of the whole areas of water lakes in the world (Ismailova, 2004). Although 130 rivers enter this basin, approximately 80% of river runoff belongs to the Volga, compared to 6% and 3% for Kura and Ural respectively (Kosarev and Yablonskaya, 1994; Kosarev, 1975). Figure 1 shows the location and some important features of this Sea.

In general, currents of the Caspian Sea are a result of wind, density differences, and river runoff. Among all factors, atmospheric forcing plays a pivotal role to form currents in this basin. Initially, in 1959 atmosphere circulation over this basin was categorized into 13 groups, although it was converted into two categories in present time (Kostianoy et al., 2005). In this categorization, the first group includes strong northerly winds, which constitute roughly 41% of all atmosphere circulation, and nearly half of this wind pattern is north westerly. The second group is the southerly winds related to cyclonic westerly wind circulation. Compared to the ocean that is located at the same latitude, the mean temperature of the Caspian Sea is 1-2 degrees lower than open oceans, whereas the mean salinity of this lake is only one-third compared to that of open oceans (Kostianoy et al., 2005). The warmest and coldest month are January and July (or August in some parts) respectively. These days, this area is much more important because of oil and gas extraction, leading to some problems in this area such as oil contamination and global warming.

Some researchers have tried to address the physical oceanography processes of the Caspian Sea using observation data, satellite images, as well as numerical modelling simulations. Among them, in recent years, Ibrayev et al. (2010) utilized three-

\*Corresponding author:

bidokhti@ut.ac.ir

dimensional numerical models to investigate seasonal circulation and water mass transport. They successfully simulate sea level and also heat and moisture fluxes variability for four coastal points. HYCOM model is used by Kara et al. (2010) to study the circulation and the effects of river discharge on seasonal salinity distribution of the Caspian Sea. The existence of temporal eddies on the southern basin was also an important result of this research. In addition, Gunduz and Özsoy (2014) applied numerical models to study the surface circulation and thermohaline structure. The result of this paper indicates that there is cyclonic circulation in the middle basin in winter, while cyclonic and anticyclonic circulations are observable in the southern basin of the Caspian Sea. This type of research was continued by Shieh et al. (2016). They used the COHERENS model to carry out simulations on water surface circulation in the Caspian Sea. They show that the thermocline in the southern basin starts at depth of about 30-40 m and 10-20 m in fall and spring respectively. In addition, Komijani et al. (2019) utilized ROMS model to study changes in seasonal circulation of the Caspian Sea focusing on air-sea interaction. The results of this study indicated that there was a temporal weak northward

current on the eastern coast as compared to a permanent strong southward current on the west coast of this Sea. Babagoli Matikolaei et al., (2019) and Babagoli Matikolaei and Aliakbari Aliakbari Bidokhti (2019) have also concentrated on the formation of deep abyssal currents in the Caspian Sea, using numerical modelling and an analytical model. They investigated the behaviour of dense flow near the Iranian coast, which shows that two eddies can form in deep water in the vicinity of Sepidrud Cape. This study is expanded by laboratory-based research, which has been done in the GFD laboratory at the University of Tehran to simulate dense flow behaviours in the stratified environment (Babagoli Matikolaei and Aliakbari Bidokhti, 2019). This study showed that two eddies can form in the vicinity of the Sepidrud Cape, named Seddy (Sepidrud cyclone eddy) and Anseddy (Sepidrud anticyclone eddy).

The present research tries to study the effect of atmospheric forcing on the physical process of the Caspian Sea, although the investigation of eddies' behaviours is the main goal of this paper. Here, we utilize a numerical model to address the physical oceanography mechanism of this Sea. The results will be discussed and the impacts of each phenomenon will be mentioned in the conclusion section.

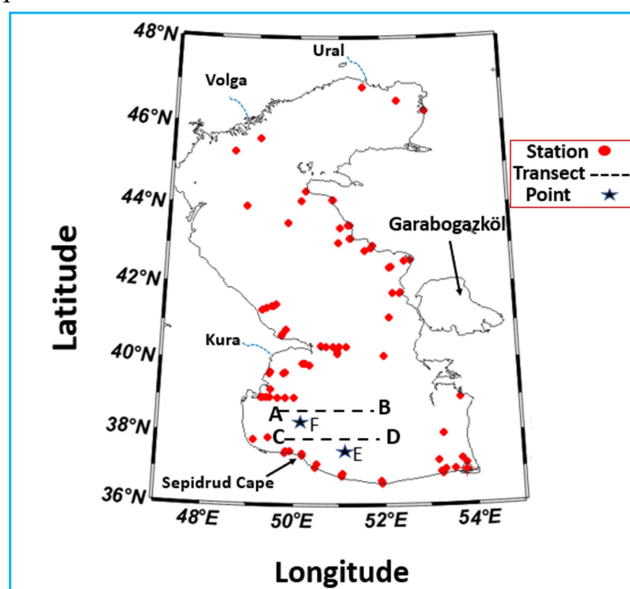


**Figure 1.** Schematic diagram of the Caspian Sea illustrating the locations of the significant rivers including Volga, Ural, Kura, Sepidrud Cape and the Garabogazköl Gulf. The locations of the CTD data are marked in red, which are used to validate the result of the model. The CTD casts are for nearly 90 stations for the fall of 2001, which are downloaded from NOAA ([www.noaa.gov](http://www.noaa.gov)). Some transections (A-B and C-D), and two points (star symbols) are marked in this figure, which will also be used for transect study later in the paper. The figure is plotted by ODV (Ocean Data view) software that is downloaded from [odv.awi.de](http://odv.awi.de).

## 2. Model Configurations

HYCOM is a capable numerical model used in oceanography research for simulating various phenomena. The model is a hydrostatic, primitive equation general circulation model (Halliwell, 2004; Savage et al., 2015). This model can work with all three z-level, sigma, and isopycnal coordinate systems due to different situations, and also HYCOM apply Arakawa C-grid method for simulating the momentum equation components. This model uses finite-differencing of Boussinesq Navier–Stokes equations (Bleck, 2002).

This model is capable to work both in shallow and deep water (Yao and Johns, 2010; Rahnemania et al., 2018). HYCOM was presented by Bleck et al. (1992) to substitute the previous model such as Miami Isopycnic-Coordinate Ocean Model (MICOM). The implementation of the generalized vertical coordinate in HYCOM is based on theoretical concepts set in Bleck and Boudra (1981) and Bleck and Benjamin (1993). The hybrid coordinates in HYCOM can be isopycnic in the open and stratified ocean, converting to sigma in shallow water. Due to the capabilities of this model in both shallow and deep water, this model can be suitable in all north, middle and south basins of the Caspian Sea. There are five algorithms, two of which are related to bulk models and others are continuous differencing schemes. HYCOM can be classified as a Lagrangian Vertical Direction (LVD) model that solves the continuity equation prognostically throughout the domain, while the Arbitrary Lagrangian-Eulerian (ALE) technique is applied to remap the vertical coordinate and maintain various coordinate types in the domain (Chassignet et al., 2007; Adcroft and Hallberg, 2006). In HYCOM, the continuous differencing model includes Mellor-Yamada 2.5, GISS and KPP. Vertical mixing can be obtained by these model schemes, while the bulk model includes PWP and Kraus-Turner (Chassignet et al., 2006). The model equations include momentum, continuity, and thermodynamics variables, which are written based on  $x$ ,  $y$ , and  $\xi$  coordinates. These equations are as follows:

$$\begin{aligned} \frac{\partial \vec{V}}{\partial t} + \nabla_{\xi} \frac{\vec{V}^2}{2} + (\zeta + f)\hat{k} \times \vec{V} + \left( \xi \frac{\partial p}{\partial \xi} \right) \frac{\partial \vec{V}}{\partial p} + \\ \nabla_{\xi} M - p \nabla_{\xi} \alpha = -g \frac{\partial \vec{\tau}}{\partial p} + \left( \frac{\partial p}{\partial \xi} \right)^{-1} \nabla_{\xi} \cdot \left( v \frac{\partial p}{\partial \xi} \nabla_{\xi} \vec{V} \right) \\ \frac{\partial}{\partial t} \left( \frac{\partial p}{\partial \xi} \right) + \nabla_{\xi} \cdot \left( \vec{V} \frac{\partial p}{\partial \xi} \right) + \frac{\partial}{\partial \xi} \left( \xi \frac{\partial p}{\partial \xi} \right) = 0 \\ \frac{\partial}{\partial t} \left( \frac{\partial p}{\partial \xi} \theta \right) + \nabla_{\xi} \cdot \left( \vec{V} \frac{\partial p}{\partial \xi} \theta \right) + \frac{\partial}{\partial \xi} \left( \xi \frac{\partial p}{\partial \xi} \theta \right) = \\ \nabla_{\xi} \cdot \left( v \frac{\partial p}{\partial \xi} \nabla_{\xi} \theta \right) + \Pi_{\theta} \end{aligned} \quad (1)$$

where  $\vec{V} = (u, v)$  is the horizontal velocity vector,  $\xi$  is one of the vertical coordinates,  $p$  and  $\theta$  are pressure and any model's thermodynamic variables (temperature and salinity).  $\zeta = \frac{\partial v}{\partial x_{\xi}} - \frac{\partial u}{\partial y_{\xi}}$  is the vertical component of relative vorticity,  $\alpha = \rho \theta^{-1}$  is a potential specific volume. Also,  $M = gz + p\alpha$  is the Montgomery potential, where  $gz = \Phi$  is geopotential. In Equation (1),  $f$  is the Coriolis parameter and  $\hat{k}$  is the vertical unit vector.  $v$  and  $\vec{\tau}$  are the eddy viscosity (or diffusivity) coefficients and the wind (or bottom) drag induced shear stress vector respectively.  $\Pi_{\theta}$  is the sum of diabatic source terms including diapycnal mixing acting on  $\theta$  fields, where  $\dot{\xi}$  shows the time derivative. For more details of equations see Wallcraft et al. (2003) and Bozec (2013).

In this study, HYCOM model is used to simulate some physical features of the Caspian Sea. For bathymetry data, we used GEBCO (General Bathymetric Chart of the Oceans) with a resolution of 30 seconds ([www.gebco.net](http://www.gebco.net)). To enhance the model performance and minimizing integral errors, we overlook the regions with depths below 1 m. Also, the interpolation technique is used with some smoothing methods to decrease the steepness of topography. The special resolution of the model is considered  $0.04^{\circ}$  which can be approximately 3.2 km based on the Mercator projection. As the Caspian Sea is a closed basin, there is not any open boundary in model set-up, except for atmosphere forcing. Tidal forcing is not applied to model because the effect of that is negligible in this basin. To apply initial conditions, the World Ocean Atlas data ([www.nodc.noaa.gov](http://www.nodc.noaa.gov)) is used. The initial data are validated by comparing with numerical modelling outputs like Kara et al.

(2010). The validations of input data indicated that the temperature data is rational and we applied the model without any changes. However, the salinity data is much higher than the salinity, which was shown by the outputs of Kara et al (2010). To interpolate the salinity data, we used MATLAB codes to the data and then we applied the salinity in the model. It would be very important as the changes in salinity is at very low rate in the Caspian Sea, which leads to more running time so that the model showed the accurate salinity of the Caspian Sea, shown by observations. For the river runoff, monthly data are extracted from the Global Runoff database. Although there are many rivers, the largest river, namely Volga, Kura and Ural rivers data applied in the model. One-hourly NCEP-CFSV2 (<https://rda.ucar.edu>) meteorological forcing is extracted with a resolution of  $0.2^\circ$ . Air temperature, sea surface temperature, precipitation, shortwave and longwave radiation, wind stress, and sea surface pressure are some forcing variables. Due to weak stratification particularly in the southern basin deeper part, 25 vertical layers are selected after some trial and errors. The simulations include the use of Mellor-Yamada level 2.5 turbulence closure scheme, which was firstly used in the Princeton Ocean Model (Mellor and Yamada, 1982; Mellor, 1998). Although the eddy diffusivity is parameterized in Mellor and Yamada method, the mean typical value for the eddy diffusivity can be considered roughly  $10^{-4}$ - $10^{-3}$   $\text{m}^2/\text{s}$  (for more details, please see Deleersnijder et al. (2008)). In this simulation, the drag coefficient is considered  $1.1 \times 10^{-3}$  for bottom friction.

The model was run for 18 years from 1992 to 2009. In this period, the model warm-up is estimated roughly as 5 years after plotting salinity time series. The baroclinic and barotropic time step is 180 and 18 sec, respectively. Given the stability of the model, these values are considered so that the CFL condition is satisfied. The model became unstable at higher time steps, so we selected this time step after utilizing trial and errors and considering the stability equation. In general, the shallow waters of the North Caspian Sea can be one of the main reasons for the instability of the model. Compared to

other works, we boost the running time, while the optimum resolution of the data is applied in the model.

### 3. Results

Initially, many temperature, salinity, and density fields are plotted to evaluate the physical oceanography properties of the Caspian Sea (Figures 2 and 3). Then, to validate the result of the model, some observational data are used; these data were collected for the autumn of 2001, which are extracted from [www.nodc.noaa.gov](http://www.nodc.noaa.gov) (Figure 4). The comparison of the model simulations and observational data shows that the model results are in appropriate forms. When it comes to salinity, the accuracy of the model is very satisfactory. Interestingly, in the vicinity of the Sepidrud Cape, the observation only shows low salinity waters as the existence of the Sepidrud River. This is mainly because we ignore the discharge of this river in the model as it is not large compared to the two larger rivers, namely Volga and Kura. Also, the salinity in the observation is a little higher than the model outputs in some parts, particularly over the Apsheron sill as the Garabogazkol Gulf is not considered in the simulation. This region is the main source of salinity in this basin due to the high evaporation. However, some differences between temperature observations and the model outputs are observable in the mean temperature for autumn, plotted using model outputs, but the observation data was collected in a different time (days or nights) of autumn. In general, the number of measuring stations is very limited to compare the model result with observation in more details. This limitation can be one of the reasons as to why we run the model for this sea. In addition to validate with observation data, we compared the model output with other research in this area. For example, there are many similarities between hydrodynamics features in our work and Gunduz and Özsoy (2014), particularly in temperature and salinity. However, the present model showed much better circulation and eddy structures compared to the model done by Gunduz and Özsoy (2014). For example, it would be a little difficult to distinguish the structure of two eddies from each other (e.g., Figure 8 in

Gunduz and Özsoy (2014)), while we can easily realize the structure of two eddies with each other in the present study due to the resolution of the model. The result of temperature, salinity, and density indicates that the temperature effect is much more important on the water density structure. Based on the model output, the range of

temperature varies from 0 to 30 degree, which is remarkable in the northern part. In comparison to this, the salinity changes from 10 to 13 PSU in the southern part of the Caspian Sea, except for the vicinities of rivers. In the northern part of the Caspian Sea, the mean salinity can be estimated roughly as 6-7 PSU.

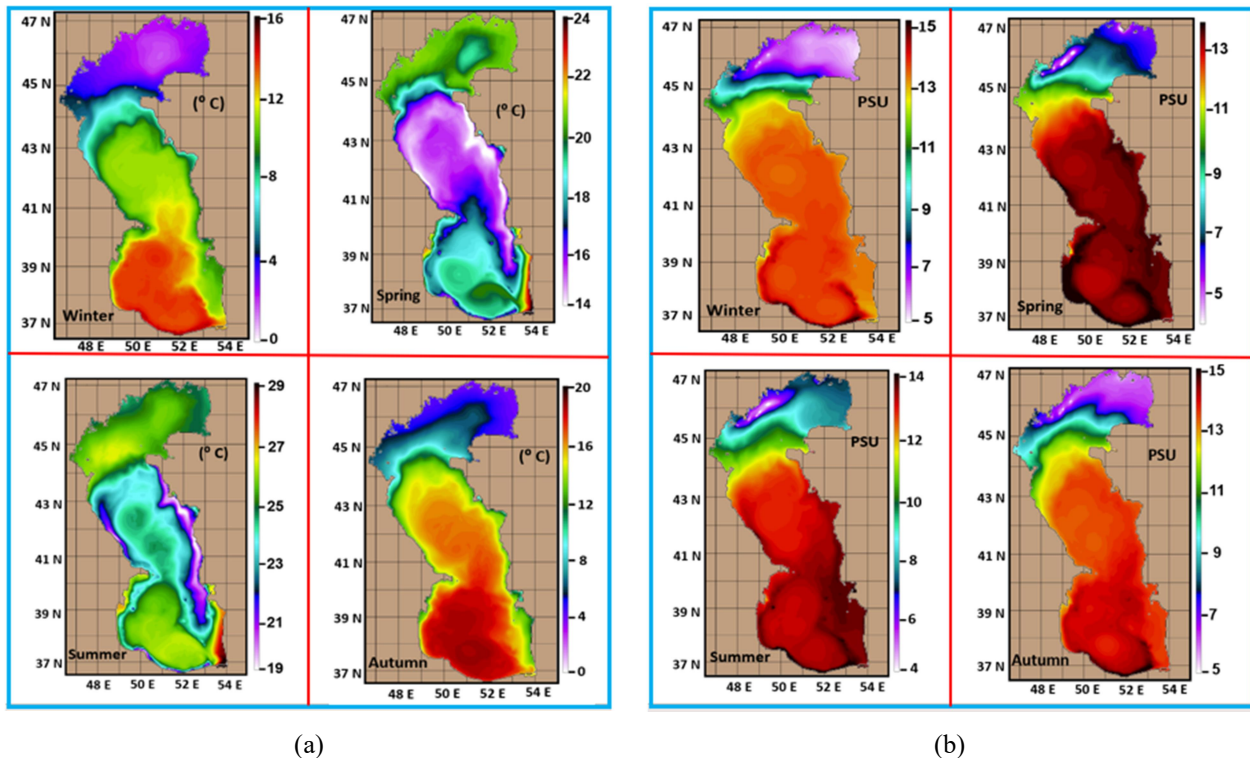


Figure 2. (a) The mean seasonally sea surface temperature in degree Celsius, (b) The mean seasonally sea surface salinity in PSU. All data are for the year of 2009 based on model simulations.

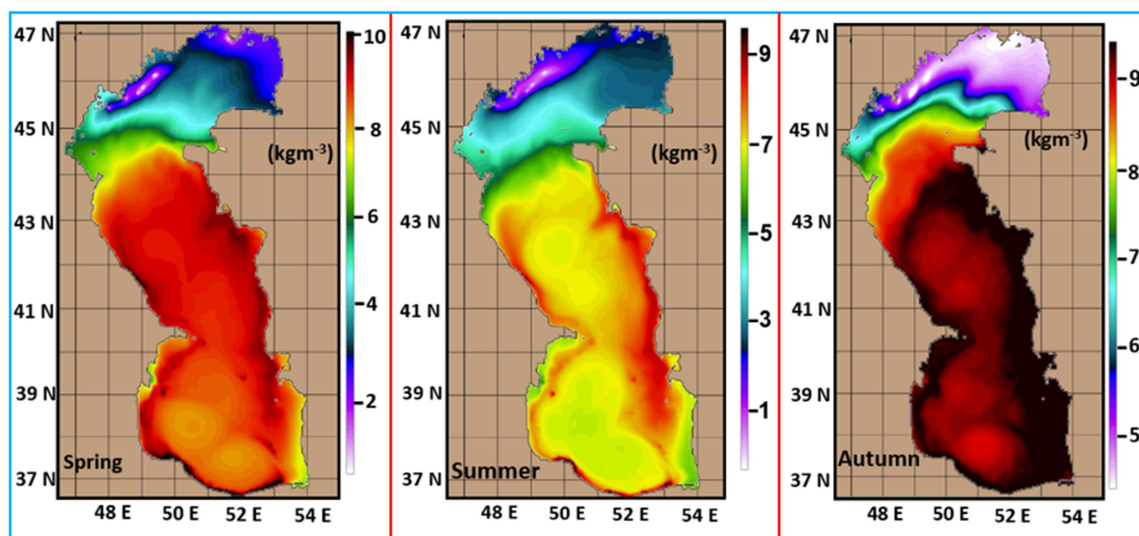
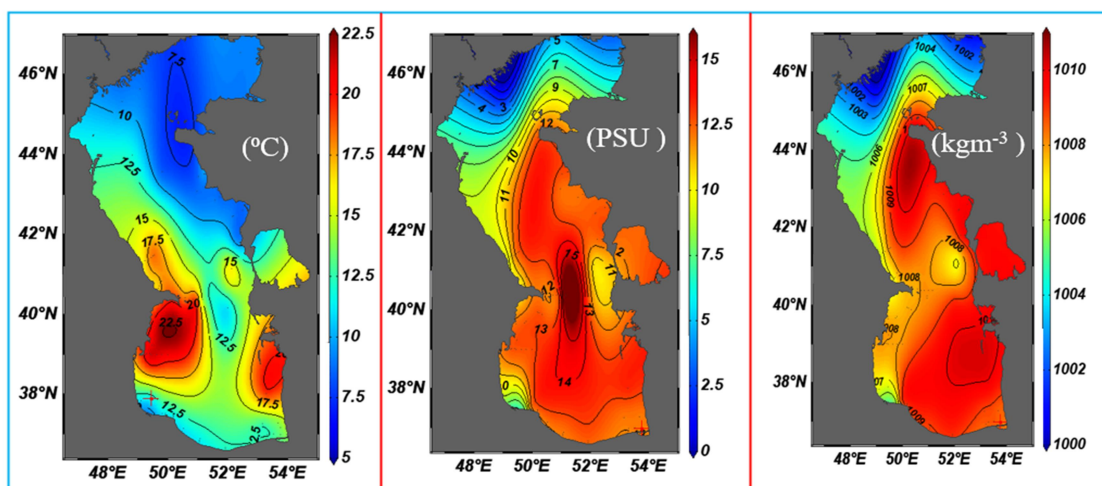


Figure 3. The mean sea surface density (sigma-theta) for some seasons in kg/m<sup>3</sup> for the whole domain in the year 2009.



**Figure 4.** Temperature, salinity, also density fields based on some observational data for autumn 2021. These figures are plotted using roughly 90 stations. The stations are shown in Figure 1. MATLAB software is utilized for interpolation and plotting.

The temperature field shows that upwelling phenomena occur in the north-eastern side of the middle basin, particularly in the summer. The cold-water pumped from deeper water towards surface water by the north-easterly wind, leading to a lower temperature in surface water in the coastal area of the eastern area. Interestingly, the coastal line, which shows the upwelling area, can be estimated up to 300 km, although in the western part this phenomenon can be observable in limited months of the summer. On the other hand, the cold water sinking process occurs in the northern basin, which is very important in the ventilation of the deep parts in this basin. This phenomenon occurs in the northern part, particularly in the cold season at the end of falls and the arrival of winters. The existence of cold weather leads to increasing surface density. The dense water overturns to deep parts and forms the abyssal water in the Caspian Sea. The formation of ice and brine rejection accelerates this phenomenon in December and January.

Here, we try to understand the mechanism of eddies when forming in the Caspian Sea. For this purpose, initially, some streamlines in different months are plotted for deeper areas for the understanding of circulation patterns in the whole parts of the Caspian Sea (Figure 5). In general, in the northern part, limited eddying activity is observable as compared to other parts. In the middle basin, one cyclone eddy is formed and endures in most months

of the year. The radius of this eddy varies from 33 km to 100 km, and the radius of this eddy can reach 75 km and 47 km in winter and spring respectively. Also, the radius of this eddy in December is about 100 km when it is strongest as compared to its mean radius of 55 km in summer. In addition, the maximum eddies in middle can reach up to five smaller ones in the limited months of the year. However, in the southern part, there are four eddies that form dipoles in January with a typical radius of 60 km for the largest cyclonic eddy. The number of eddies increases in February, particularly between latitudes 39 and 40 degrees with smaller scales. The cyclonic eddies are stronger with a radius of roughly 50 km, although many sub-mesoscale eddies are observable. In August, while two of the mesoscale eddies are cyclone, one of them is anticyclone. In the fall, the strongest eddies are observable in December, with a radius of about 70 km. The bottom topography of the Caspian Sea certainly affects the distributions of these eddies, and it seems that the deeper middle and southern parts encompass the larger eddies, mainly in the western sides of deep basins of the sea. Hence topographic steering effect ( $f/H \approx \text{constant}$ , where  $f$  is Coriolis parameter and  $H$  is water depth) is strong in this enclosed sea.

For a better understanding of eddy's behaviours, some transects are plotted along some longitudes (Figures 6 and 7). Velocity transects show that while orbital velocity can

be estimated up to 8 cm/s, the associated zonal velocity is roughly 35 cm/s. These eddies can affect water up to 400 m deep, but the greatest effect can be observable below 200 m. Among all months, the minimum velocities associated with eddies are for August. In addition, the time series of salinity is plotted to investigate the trend of this parameter throughout the year when eddy is forming in the southern basin. The time series show different behaviours for cyclonic and anticyclonic eddies. The remarkable fluctuations of time series in different seasons completely show the longevity of eddy in different seasons. Whereas the changes of salinity for cyclonic eddies can be 0.1 PSU, this value for anticyclonic

eddy is 0.12 PSU. Based on the locations of E and F (Figures 1 and 5), we can understand which eddies are cyclonic or anticyclonic eddies. April and May are months in which salinity is almost the same for both types of eddies in the southern basin. In other months, for example, from December to May, the salinity of cyclonic eddies is slightly higher than that of anticyclonic eddies. In other months, this trend is reversed. Surface salinity structural variations are also more pronounced in warm seasons, especially summer (Figure 8), as surface precipitated fresh water is less and evaporation is larger over the basin in these months. Hence, eddies salinity structures are more pronounced.

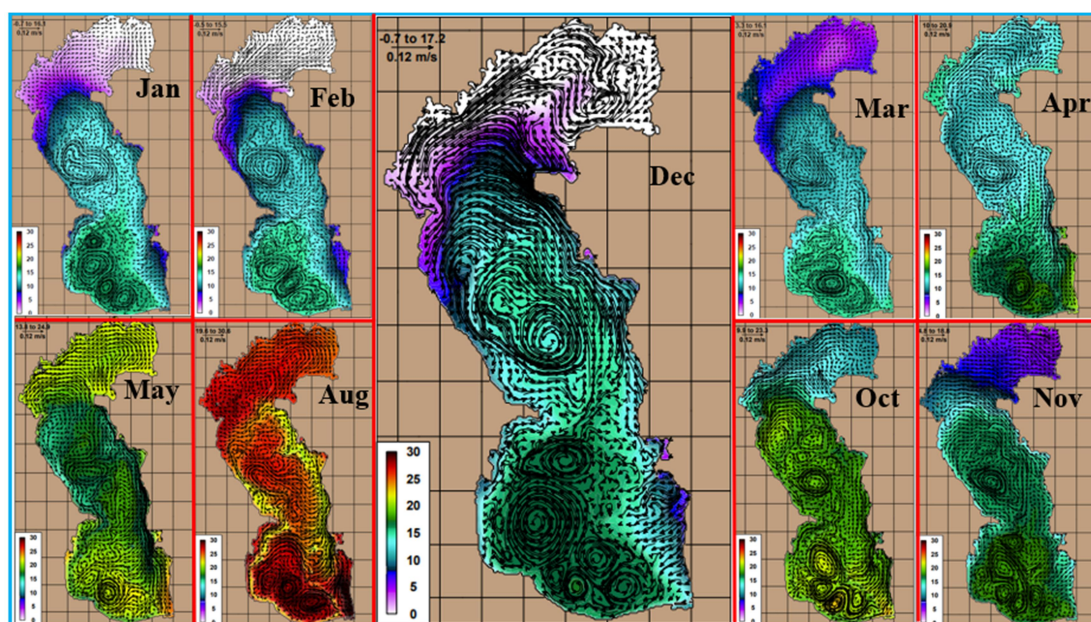


Figure 5. Streamlines in the Caspian Sea for different months, while the background is temperature. The colour bar shows the temperature in degree Celsius.

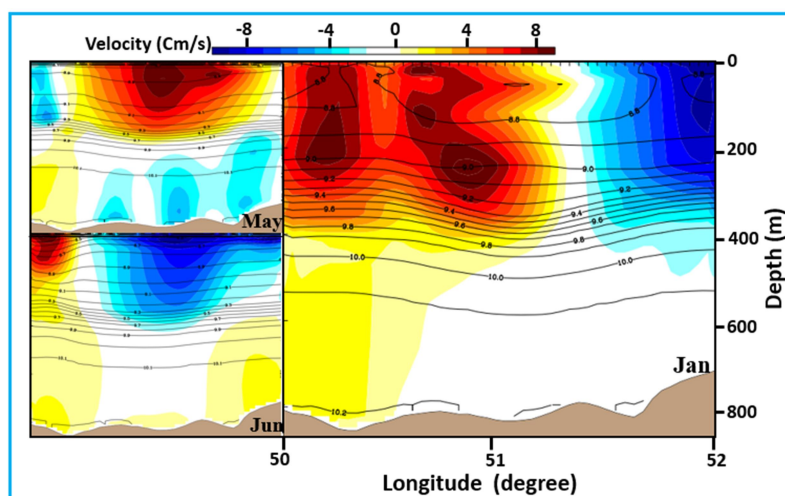
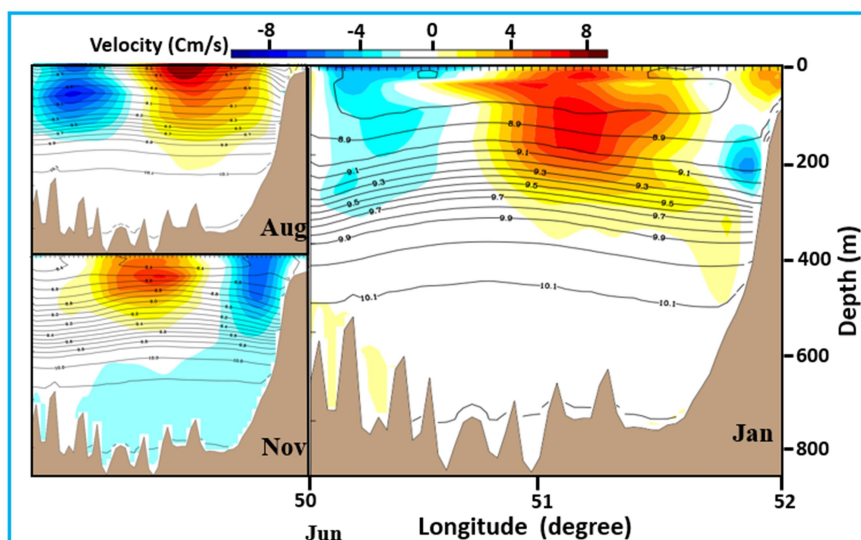
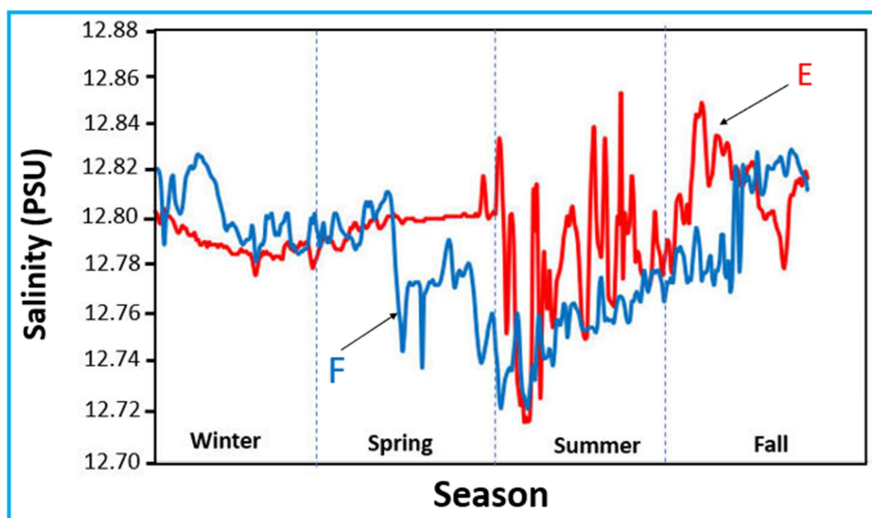


Figure 6. The meridional velocity transects across longitude based on cm/s. For the location of this transect, see transects C-D in Figure 1. Contours are sigma-theta.



**Figure 7.** The same as Figure 6 but for transect A-B in Figure 1. The eddies can be understood from the colour (velocity) when blue (negative velocity) and red (positive velocity) shows the structure of eddies.



**Figure 8.** Time series of salinity during different seasons for two surface points in the southern part of the Caspian Sea. The locations of E and F are shown in Figure 1.

#### 4. Summaries and Conclusion

This study investigated some physical properties of mesoscale eddies in the Caspian Sea, using numerical simulations by HYCOM model and some observations. The main aim of this paper was to study the behaviours of mesoscale eddies in the Caspian Sea under different seasonal changes. We monitored temperature, salinity and density fields in this enclosed sea because of two reasons. Firstly, we tried to evaluate the accuracy of our model when comparing simulation results with observational data. Secondly, the simulations gave us an opportunity to understand the physical properties of eddies sizes and

structures. This can be beneficial in oceanography as we can understand the source of instability. For example, the temperature structure creates instabilities in some current like the Gulf Stream, when warm centres (anticyclonic) and cold centres (cyclonic) are formed. In the Persian Gulf, salinity structure is the main cause of instability (Rahnemania et al., 2019).

Also, in considering the temperature, salinity and also density of this sea, the results indicated that upwelling and sinking can occur on the eastern part of the middle basin and northern basin respectively. The main reason for the occurrence of these phenomena is the direction of the wind that is

north-easterly in July, although this phenomenon is weaker in other months of summer. The vertical velocity can be estimated up to  $10^{-5}$  m/s for sinking and upwelling. However, in the north basin when the weather became cold, the water density increases, leading to overturning in the north part of the central basin of the Caspian Sea. This phenomenon is the main reason for the thermohaline circulation in the Caspian Sea, which leads to the ventilation of the deep water of this lake. The vertical structures of eddies with sinking and upwelling processes were also considered. Anticyclonic eddies show behaviours similar to the downwelling process (negative vertical velocity), while cyclonic eddies tend to produce upwelling.

The results show that many eddies with different scales can occur in the Caspian Sea. However, Cyclonic eddies in the middle basin, and two cyclonic and one anticyclonic eddy in the southern parts are the main eddies of the Caspian Sea. To summarize the locations and sizes of eddies that are formed in the Caspian Sea, we plot schematically, the most important eddies in Figure 9 based on the real size and the rotation direction of eddies using model simulations. Interestingly, whereas a cyclonic eddy form in the middle basin, most of eddies in the southern basin form one or two dipole eddies. Among them, one cyclonic and anticyclonic eddies appear to be rather permeant eddies that are formed over the deeper parts of the middle and southern basins of the Caspian Sea. Hence, it appears that the bottom topography governs the formations of the main eddies. The main eddies tend to be on the western side of this Sea. Also, it seems that the instability which leads to forming both types of eddy can be for two reasons. Firstly, the prevailing wind field inducing surface currents that moves southwards towards the Iranian coast. Secondly, the topography of the Sepidrud Cape causes instability of the current, forming eddies. It goes without saying that the Coriolis force is the main parameter to form these eddies as the Rossby number is small for this type of phenomena. In terms of dynamics of eddies,

the Rossby number ( $R_0 = \omega/f$ ;  $\omega$  is relative vorticity and  $f$  Coriolis parameter) for the southern part eddies can be estimated roughly 0.08, which shows importance of Coriolis effects. In addition, Burger number ( $Bu = \frac{NH}{\Omega L}$ ;  $N$  is Buoyancy frequency,  $\Omega$  angular rotation rate of the earth,  $H$  is the height scale,  $L$  is a horizontal length scale) can be calculated roughly 0.2 for these eddies, which shows the importance of rotation compared to the density stratification (Kurien and Smith, 2012).

Interestingly, these eddies have formed in the regions off the coast of the southern Caspian Sea along the continental-shelf. It means that the topography mainly controls the formation of eddies, especially in the southern basin. The large-scale eddies are mainly situated over the deeper parts, extending to depths of 400 to 500 m.

When comparing the result of this paper with other researches, we can conclude that the present simulation clearly shows the behaviours of eddies with higher resolution, as we have used a more appropriate running time and high-resolution forcing data in these simulations.

The main reasons why these mesoscale eddies are very important in the southern basin is the issue of oil contamination (Aladin and Plotnikov, 2004). The authors consider that these eddies may be the main reasons why the western part of the southern basin is a more polluted area compared to the eastern region of the Caspian Sea. To support our visions, Mirzaei et al. (2014) and Babagoli Matikolaie (2021) showed that the vicinity of Sepidrud Cape is the most polluted area in terms of oil pollution in most months of the year. With these findings on eddies activities, this pollution is expected in this area as these eddies have capabilities to transport heat, pollution and other biomaterials. These eddies can transport contaminated waters from Apsheron sill area with many oil exploration activities to this area. Hence, the authors believe that this finding can be addressed in some marine pollution problems in this enclosed and vulnerable large lake.

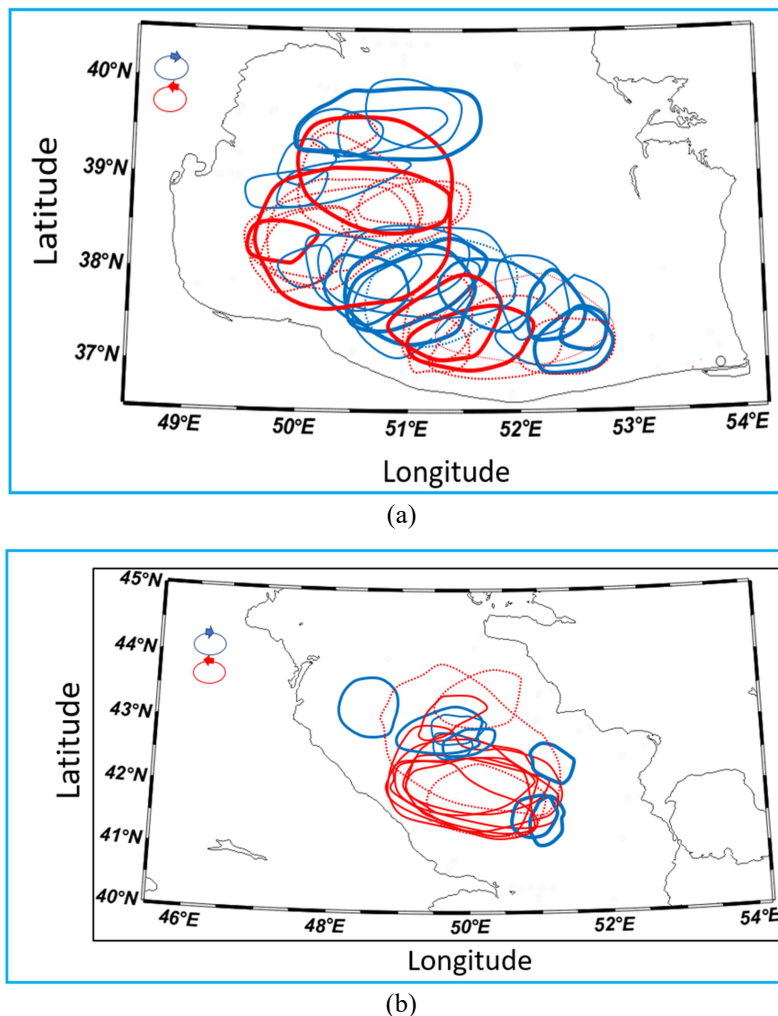


**Figure 9.** Summary of the locations of the formations and paths of eddies in all months. These figures are plotted to show the location and size of eddies and also the rotation of them, which are observable in the present work. a and b are for the southern and middle basins, respectively. The blue colour refers to cyclonic eddies whereas the red colour belongs to areas of anticyclonic eddies. The extensions of eddies are presented by solid or dotted lines to show them more clearly.

## References

- Adcroft, A. and Hallberg, R., 2006, On methods for solving the oceanic equations of motion in generalized vertical coordinates. *Ocean Modelling*, 11(1-2), 224-233.
- Aladin, N. and Plotnikov, I., 2004, The Caspian Sea. Lake Basin Management Initiative. 29 p.
- Aubrey, D.G., 1994, Conservation of biological diversity of the Caspian Sea and its coastal zone, A proposal to the Global Environment Facility, Report to GEF.
- Aubrey, D.G., Glushko T.A. and Ivanov, V.A., 1994, North Caspian Basin: Environmental status and oil and gas operational issues, Report for Mobil-oil 650 pp.
- Babagoli Matikolaei, J., Aliakbari Bidokhti, A. and Salmani Ghazvini, Z., 2017, Investigation of physical properties and long coastal waves in the southern Caspian Sea. *Iranian Journal of Geophysics*, 12(3), 39-52.
- Babagoli Matikolaei, J. and Aliakbari Bidokhti, A.A., 2019, An experimental study of flow regimes of a gravity current over a Cape in a stratified environment. *Ocean Dynamics*, 69(7), 769-786.
- Babagoli Matikolaei, J., Aliakbari Bidokhti, A. and Shiea, M., 2019, Some aspects of the deep abyssal overflow between the middle and southern basins of the Caspian Sea. *Ocean Science*, 15(2), 459-476.
- Babagoli Matikolaei, J., 2021, Impact of

- physical process on propagating oil spills in the Caspian Sea. *Marine Pollution Bulletin*, 165, 112147.
- Bleck, R. and Benjamin, S.G., 1993, Regional weather prediction with a model combining terrain-following and isentropic coordinates. Part I: Model description. *Monthly Weather Review*, 121(6), 1770-1785.
- Bleck, R. and Boudra, D.B., 1981, Initial testing of a numerical ocean circulation model using a hybrid (quasi-isopycnic) vertical coordinate. *Journal of Physical Oceanography*, 11(6), 755-770.
- Bleck, R., Rooth, C., Hu, D. and Smith, L.T., 1992, Ventilation patterns and mode water formation in a wind-and thermodynamically driven isopycnic coordinate model of the North Atlantic. *Journal of Physical Oceanography*, 22(12), 1486-1505.
- Bleck, R., 2002, An oceanic general circulation model framed in hybrid isopycnic-Cartesian coordinates. *Ocean modelling*, 4(1), 55-88.
- Bozec, A., 2013, Hybrid Coordinate Ocean Model. HYCOM for Dummies.
- Chassignet, E.P., Hurlburt, H.E., Smedstad, O.M., Halliwell, G.R., Hogan, P.J., Wallcraft, A.J. and Bleck, R., 2006, Ocean prediction with the hybrid coordinate ocean model (HYCOM). In *Ocean weather forecasting*, 413-426, Springer, Dordrecht.
- Chassignet, E.P., Hurlburt, H.E., Smedstad, O.M., Halliwell, G.R., Hogan, P.J., Wallcraft, A.J. and Bleck, R., 2007, The HYCOM (hybrid coordinate ocean model) data assimilative system. *Journal of Marine Systems*, 65(1-4), 60-83.
- Deleersnijder, E., Hanert, E., Burchard, H. and Dijkstra, H.A., 2008, On the mathematical stability of stratified flow models with local turbulence closure schemes. *Ocean Dynamics*, 58(3-4), 237-246.
- Gill, A.E., 1983, Eddies in relation to climate. In: Robinson AR (ed) *Eddies in marine science*. Springer Verlag.
- Gunduz, M. and Özsoy, E., 2014, Modelling seasonal circulation and thermohaline structure of the Caspian Sea. *Ocean Science*, 10(3), 459-471.
- Halliwell, G.R., 2004, Evaluation of vertical coordinate and vertical mixing algorithms in the HYbrid-Coordinate Ocean Model (HYCOM). *Ocean Modelling*, 7(3-4), 285-322.
- Ibrayev, R.A., Özsoy, E., Schrum, C. and Sur, H.I., 2010, Seasonal variability of the Caspian Sea three-dimensional circulation, sea level and air-sea interaction. *Ocean Science*, 6(1), 311-329.
- Ismailova, B.B., 2004, Geo-information modeling of wind-induced surges on the northern-eastern Caspian Sea, *Math. Comput. Simulat.*, 67, 371-377.
- Kara, A.B., Wallcraft, A.J., Metzger, E.J. and Gunduz, M., 2010, Impacts of freshwater on the seasonal variations of surface salinity and circulation in the Caspian Sea. *Continental Shelf Research*, 30(10-11), 1211-1225.
- Komijani, F., Chegini, V. and Siadatmousavi, S.M., 2019, Seasonal variability of circulation and air-sea interaction in the Caspian Sea based on a high-resolution circulation model. *Journal of Great Lakes Research*, 45(6), 1113-1129.
- Kosarev, A.N., 1975, The hydrology of the Caspian and Aral Seas. *Mosk. Gos. Univ., Moskva (USSR)*, 272.
- Kosarev, A.N., 1990, The Caspian Seawater structure and dynamics. *Nauka, Moscow (in Russian)*.
- Kosarev, A. and Yablonskaya, E., 1994, *The Caspian Sea*, SPB Academic Publishing, Hague.
- Kostianoy, A.G. and Kosarev, A.N. (Eds.), 2005, *The Caspian Sea environment (Vol. 5)*. Springer Science & Business Media.
- Kurien, S. and Smith, L.M., 2012, Asymptotics of unit Burger number rotating and stratified flows for small aspect ratio. *Physica D: Nonlinear Phenomena*, 241(3), 149-163.
- Mellor, G.L., 1998, *Users guide for a three-dimensional, primitive equation, numerical ocean model*. Princeton, NJ: Program in Atmospheric and Oceanic Sciences, Princeton University.
- Mellor, G.L. and Yamada, T., 1982, Development of a turbulence closure model for geophysical fluid problems. *Reviews of Geophysics*, 20(4), 851-875.
- Mirzaei, M., Moatazedi, M. and Nikbakhti, A., 2014, Scrutiny of Petroleum Hydrocarbon Pollutions in Water and

- Sediments in Southern Zone of Caspian Sea. *Journal of Natural Environment*, 67(2).
- Rahnemania, A., Aliakbari Bidokhti, A. and Babagoli Matikolaei, J., 2018, Study of ice formation in the Caspian Sea using numerical simulations. *Journal of the Persian Gulf*, 9(33), 40-0.
- Rahnemania, A., Aliakbari Bidokhti, A.A., Ezam, M., Lari, K. and Ghader, S., 2019, A Numerical Study of the Frontal System between the Inflow and Outflow Waters in the Persian Gulf. *Journal of Applied Fluid Mechanics*, 12(5), 1475-1486.
- Rodionov, S., 2012, Global and regional climate interaction: the Caspian Sea experience (Vol. 11). Springer Science & Business Media.
- Savage, J.A., Tokmakian, R.T. and Batteen, M.L., 2015, Assessment of the HYCOM velocity fields during Agulhas Return Current Cruise 2012. *Journal of Operational Oceanography*, 8(1), 11-24.
- Shieh, M., Chegini, V. and Aliakbari Bidokhti, A.A., 2016, Impact of wind and thermal forcing on the seasonal variation of three-dimensional circulation in the Caspian Sea. *Indian Journal of Geomarine Sciences*, 45(5), May 2016, pp. 671-686.
- Terziev, F.S., Kosarev, A.N. and Kerimov, A.A., (Eds.), 1992, *Hydrometeorology and hydrochemistry of Seas. Caspian Sea*, vol. VI, Hydrometeorological Conditions, issue 1. S. Petersburg, Hydrometeoizdat, 359PP (in Russian).
- Wallcraft, A., Carroll, S.N., Kelly, K.A. and Rushing, K.V., 2003, *Hybrid Coordinate Ocean Model (HYCOM) Version 2.1. User's Guide*. Naval Research Lab Stennis Detachment Stennis Space Center MS.
- Yao, F. and Johns, W.E., 2010, A HYCOM modeling study of the Persian Gulf: 1. Model configurations and surface circulation. *Journal of Geophysical Research: Oceans*, 115(C11).
- Zonn, I., Kostianoy, A.G., Kosarev, A.N. and Glantz, M.H., 2010, *The Caspian Sea Encyclopedia*. Springer-Verlag BBerlin Heidelberg. 537 pages.